

The Stellar Mass Function

Pavel Kroupa¹

*Institut für Theoretische Astrophysik, Universität Heidelberg,
Tiergartenstr. 15, D-69121 Heidelberg, Germany*

Abstract. Since the major review by Scalo (1986), significant progress has been achieved in constraining the mass function (MF) of low-mass stars. The break-throughs which today allow a much better understanding of the stellar luminosity function (LF) and the underlying MF are documented here and the resulting MF for Galactic field stars is confronted with microlensing data, the chemical enrichment history of the Galaxy, the Oort limit and well-studied open clusters.

1. Introduction

The mass, m , of an isolated main-sequence star can be determined from its absolute luminosity, l , and the mass–luminosity relation, $m(l, [\text{Fe}/\text{H}], \tau, \mathbf{s})$. The corresponding mass–(absolute-magnitude) relation is $m(M_P)$, where P represents some photometric pass band, and the other parameters have been dropped for conciseness. For Galactic disc stars with $m < 1 M_\odot$, the stellar age is usually $\tau > 1$ Gyr, $[\text{Fe}/\text{H}] > -1$ and the dependence on the stellar spin, \mathbf{s} , is not significant. The continuous distribution of stars by luminosity is related to the distribution by mass through $\psi(M_P) = -\xi(m) \times (dm/dM_P)$, where $\psi(M_P)$ and $\xi(m)$ are the LF and MF, respectively. The differential volume number density of stars in the absolute-magnitude interval $M_P + dM_P$ to M_P is $d\rho = -\psi dM_P$, which is also the differential number density of stars, ξdm , in the mass range m to $m + dm$.

The conversion of an observed LF to the MF is demonstrated in Fig. 1 using two well-cited examples from the literature. The MF is a good approximation to the initial mass function (IMF) for stars with $M_V > 5$, because they do not evolve appreciably within the age of the Galactic disc.

The mass- M_V data compiled by Henry & McCarthy (1993, hereinafter HM93) suggest that the $m(M_V)$ relations adopted by Miller & Scalo (1979, hereinafter MS) and Scalo (1986, hereinafter Sc) assign masses that may be somewhat too small for stars with $M_V \approx 10$. As shown in Section 4, theoretical work on the structure of low-mass stars confirms that there is additional structure in the $m(M_V)$ relation near this magnitude. This is an important point

¹e-mail: pavel@ita.uni-heidelberg.de; To appear in PASPC: *Brown Dwarfs and Extrasolar Planets*, R. Rebolo, M.R. Zapatero Osorio & E. Martin (eds.); International workshop held on Tenerife Island, March 17 – 21, 1997.

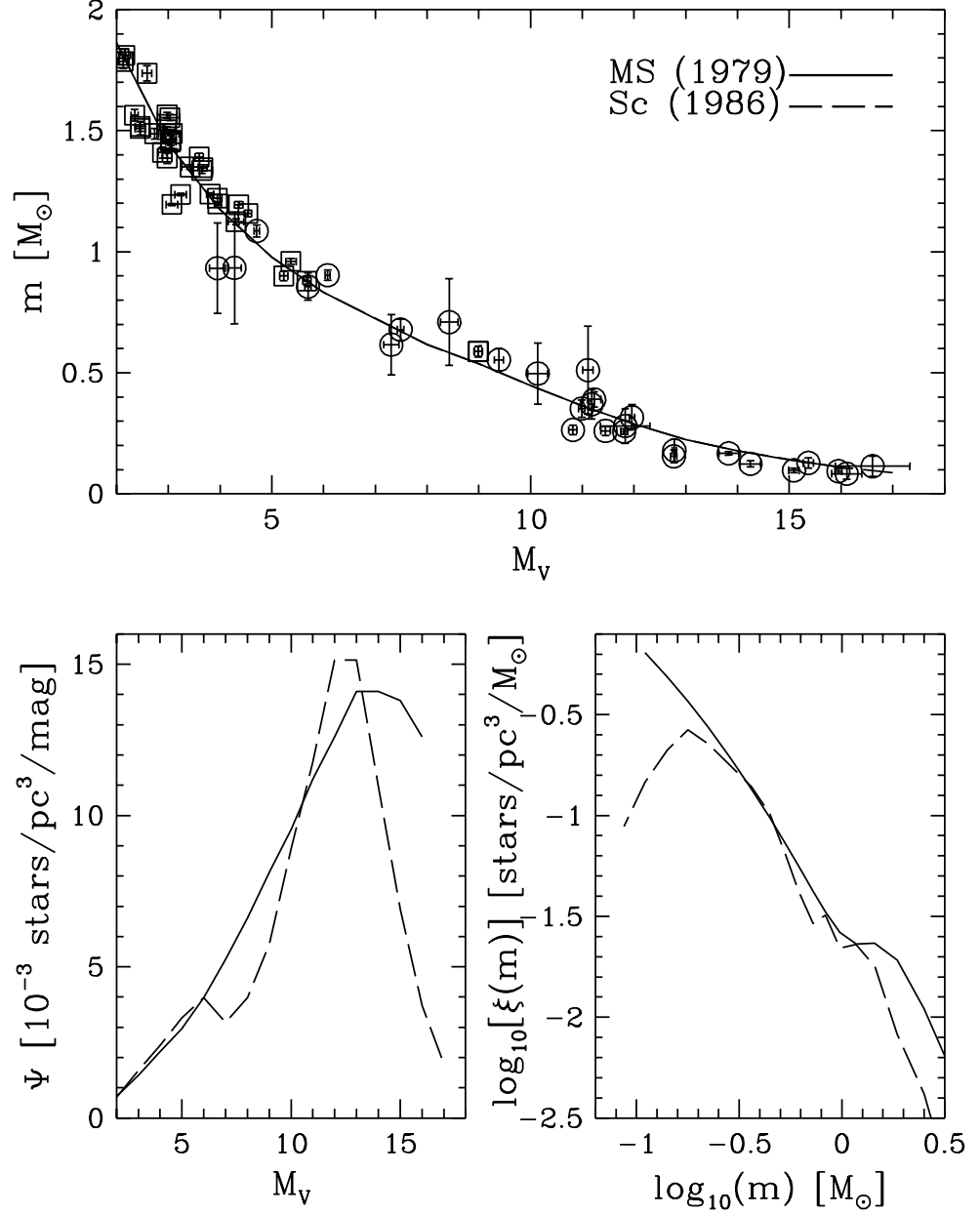


Figure 1. Upper panel: The solid and indistinguishable dashed line are the $m(M_V)$ relations used by MS and Sc, respectively. Open circles are observational data from HM93, and the open squares are from Andersen (1991). Lower panels: The stellar LF adopted by MS (solid line) and by Sc (dashed line) is shown in the left panel, and the resulting IMFs are shown in the right panel.

(D’Antona & Mazzitelli 1983, hereinafter D’AM83) because $\psi \propto dm/dM_V$, and thus any mis-understood structure in the $m(M_V)$ relation carries through to unphysical structure in the MF. The slope, dm/dM_V , becomes small at the faintest magnitudes and is not very well determined. This holds true in other photometric passbands as well (HM93) and leads to large uncertainties in the MF near the hydrogen burning mass limit.

In Fig. 1 the IMF, $\xi(m)$, is plotted as the volume number density per unit mass interval. This is obtained from the IMF, $\xi'(\log_{10}[m])$, expressed as the surface number density per unit logarithmic mass interval. It is given by Eqn. 30 in MS for a constant star formation rate and a Galactic disc age $T_0 = 12$ Gyr (their Table 7), and by Sc in his Table VII for $T_0 = 12$ Gyr. The conversion is $\xi(m) = \xi'(\log_{10}[m]) / (2hm \ln(10))$, where $2h$ is the Galactic disc thickness.

The Miller & Scalo IMF, ξ_{MS} , continues to increase down to $m \approx 0.1 M_\odot$. The Scalo IMF, ξ_{Sc} , on the other hand, has a significant maximum at $m \approx 0.2 M_\odot$. The reason for the difference is the adopted LF, measurement of which has been improved significantly between 1979 and 1986 through star-count surveys in the solar neighbourhood (Wielen, Jahreiss & Krüger 1983) and on deep photographic plates (Reid & Gilmore 1982, hereinafter RG).

Both ξ_{MS} and ξ_{Sc} have a dip near $m = 0.6 - 1.3 M_\odot$. This results because star-count data have to be corrected for the loss of the more massive stars through stellar evolution, and because h is smaller for the more massive stars. The dip can be minimised by choosing an appropriate age for the Galactic disc ($T_0 \approx 12$ Gyr) and star-formation history. For stars brighter than $M_V \approx 6$, the Galactic disc thickness decreases from $h \approx 300$ pc to $h \approx 90$ pc (e.g. Fig. 10 in Sc) leading to an enhancement of the volume density of brighter stars near the Galactic plane.

An additional reason for the dip in ξ_{Sc} is that the LF adopted by Sc shows such a feature at $M_V \approx 6-9$. This is recognised to be real (Upgren & Armandroff 1981) and a result of stellar physics (D’AM83; Kroupa, Tout & Gilmore 1990, hereinafter KTG90).

The intricate details of the transformation of an observed single-star LF to the IMF, taking account of the varying h , the birth-rate history of stars and stellar evolution, can be found in Sc and Haywood, Robin & Crézé (1997). Concerning low-mass stars, we know today that (i) the smooth $m(M_V)$ relation used by MS and Sc is not consistent with stellar models, and that (ii) the LFs adopted by MS and Sc do not correctly represent the distribution of single stars with luminosity. Consequently, the MFs plotted in Fig. 1 do not correctly describe the spectrum of stellar masses.

Since 1986, constraints on the LF have been improved (Section 2), the understanding of Malmquist bias has advanced considerably (Section 3), the observational and theoretical constraints on the mass–luminosity relation have been improved (Section 4), and the characteristics of the binary star population in the Galactic field is much better quantified (Section 5). Discussions of the MF in the substellar regime can be found in Laughlin & Bodenheimer (1993), Basri & Marcy (1997), Chabrier (these proceedings), and Jones (these proceedings). A review of the faint end of the LF can also be found in Bessell & Stringfellow (1993).

2. The Luminosity Function

Trigonometric parallaxes are used to infer the LF for the stars in the immediate neighbourhood of the Sun, where most multiple-star systems have been identified. Completeness extends, for northern declinations, to 20 pc for stars with $M_V < 9.5$, but severe incompleteness sets in beyond 5 pc for stars with $M_V > 12$ (Jahreiss 1994, Henry et al. 1997). Estimates of the nearby LF, ψ_{near} , using somewhat different sampling volumes, are provided by Wielen et al. (1983), Dahn, Liebert & Harrington (1986, hereinafter DLH) and KTG93 in the V-band, and by HM90 in the K-band. Three additional stars have been found recently within 5.3 pc: Gl 866C with $M_V \approx 15.8$ (Henry, private communication; see also Simons, Henry & Kirkpatrick 1996 and Kroupa 1995a), LP 944-20 with $M_V > 19$ (Kirkpatrick, Henry & Irwin 1997), and LHS 1565 with $M_V \approx 15.2$ (Henry et al. 1997). However, ψ_{near} remains poorly constrained for $M_V > 12$, and the contribution by faint main-sequence stars to the mass of the Galactic disc remains unclear.

Other techniques have been developed with the aim of improving the constraints on the LF at the faint end. RG made deep photographic exposures with a Schmidt telescope (see also Hawkins, these proceedings) to probe the distribution of faint main sequence stars to distances of about 100 pc. They used an automatic plate measuring machine to identify Galactic-disc red-dwarf stars from the hundred thousand images recorded on a typical Schmidt-telescope plate in the direction of the South Galactic Pole. At least two photometric pass bands are necessary to define the colours of the objects, and multiple exposures on different plates are used to confirm images. The sample of possible red dwarf stars is contaminated by red giants for typically $V - I < 1.8$, and galaxies dominate the number counts at the faintest magnitudes ($V > 19$). Distances to the stars in the final red-dwarf sample are estimated using photometric parallax. The stellar number densities are estimated taking into account the distance to which a star can be detected.

After the pioneering work by RG, other deep surveys with the method of photometric parallax explored the distribution of faint stars in different directions, Gilmore, Reid & Hewett (1985), Hawkins & Bessell (1988), Leggett & Hawkins (1988), Stobie, Ishida & Peacock (1989, hereinafter SIP) and Kirkpatrick et al. (1994). These yield *photometric* LFs, ψ_{phot} , that are consistent with each other and, after correction for Galactic disc structure, are independent of the direction of the line-of-sight through the Galactic disc. A consistent finding among these surveys, each yielding about 30–60 stars with $M_V > 12$, is that ψ_{phot} has a maximum at $M_V \approx 12$ with a decline at fainter magnitudes. That it also does not show significant variation with direction has been verified by the extensive photographic survey of Tinney, Reid & Mould (1993). The resulting LF is based on about 3500 stars spread over an area of 270 square degrees. Surveys with the Hubble Space Telescope (HST) avoid contamination by galaxies down to $V \approx 21 - 26$, and can thus probe the stellar distribution to distances of a few kpc. Santiago, Gilmore & Elson (1996) report $\psi_{\text{phot,HST}}$ based on about 20 fields and verify that ψ_{phot} decreases for $M_V > 12$. They discuss the uncertainties in $\psi_{\text{phot,HST}}$ owing to photometric calibration.

Finally, Jarrett, Dickman & Herbst (1994) constrain the faint star LF by counting 14 red stars with $M_V > 12$ that appear projected against dark molec-

ular clouds. Significant conclusions from a comparison with ψ_{near} or ψ_{phot} are not possible but the sample is also interesting because it may contain young M dwarfs that have migrated from the molecular cloud.

3. Malmquist Bias

In a colour–magnitude diagram there is scatter about the average relation, because the luminosity of a main-sequence star is a function of mass, metallicity, age and spin (Section 1). Consequently, the distance estimated from the colour and apparent magnitude of a star is subject to error. In a magnitude limited survey, such as is used to construct ψ_{phot} , this leads to overestimation of the stellar number densities because the number of stars increases with distance. More intrinsically brighter stars are counted in the photometrically defined sampling volume than intrinsically fainter stars are lost from it. This bias also leads to the resulting stellar sample appearing brighter than is typical for stars of the given colour.

SIP applied for the first time the complete Malmquist corrections to the raw photometric LF. The Malmquist correction, $\Delta\psi_{\text{phot}}/\psi_{\text{phot}} \propto \sigma_{M_P}^2$, where σ_{M_P} is the scatter about the mean absolute magnitude M_P in the colour–magnitude diagram, and is assumed to be constant and Gaussian. The cosmic scatter, σ_{M_P} , depends on the photometric bands used for photometric parallax. Using $M_I(R - I)$, rather than the shallower $M_V(V - I)$ relation, leads to significantly larger Malmquist bias (Reid 1991; Fig. 2 in Kroupa 1995a).

The detailed study of cosmic scatter in Section 3 of KTG93 shows that σ_{M_V} is non-Gaussian and a function of $V - I$, because the effects of metallicity, unresolved binaries and age lead to different, colour dependent changes in M_V . Recent progress in the modelling of realistic stellar atmospheres (Fig. 1 in Baraffe et al. 1995) qualitatively supports the metallicity model of KTG93 (their Figs. 5 and 6). Malmquist corrections are thus even more involved than the treatment by SIP.

4. The Mass–(Absolute-Magnitude) Relation

The $m(M_V)$ relation steepens near $M_V = 10$ and flattens again near $M_V = 15$, because the formation of H_2 in the outer shells of main-sequence stars causes core contraction. This leads to brighter luminosities and full convection for $m < 0.35 M_\odot$ (Chabrier & Baraffe 1997; Kroupa & Tout 1997, hereinafter KT), and to a pronounced local minimum in dm/dM_V at $M_V \approx 11.5$. Artificial suppression of H_2 formation leads to full convection at $m < 0.25 M_\odot$ and to fainter stars (KTG90, KT). In this case dm/dM_V has no significant extrema for $M_V > 9$.

This is illustrated in Fig. 2. The discussion in Section 1 implies that a minimum in dm/dM_V should correspond to a maximum in the LF, unless the MF has a minimum that cancels out the structure in dm/dM_V . All photometric LFs show a maximum near $M_V = 12$ (Section 2). The well constrained average photometric LF, $\bar{\psi}_{\text{phot}}$ (Section 6), shows this maximum to be in beautiful agreement with the theoretical $dm/dM_V(M_V)$ relation, opening the possibility

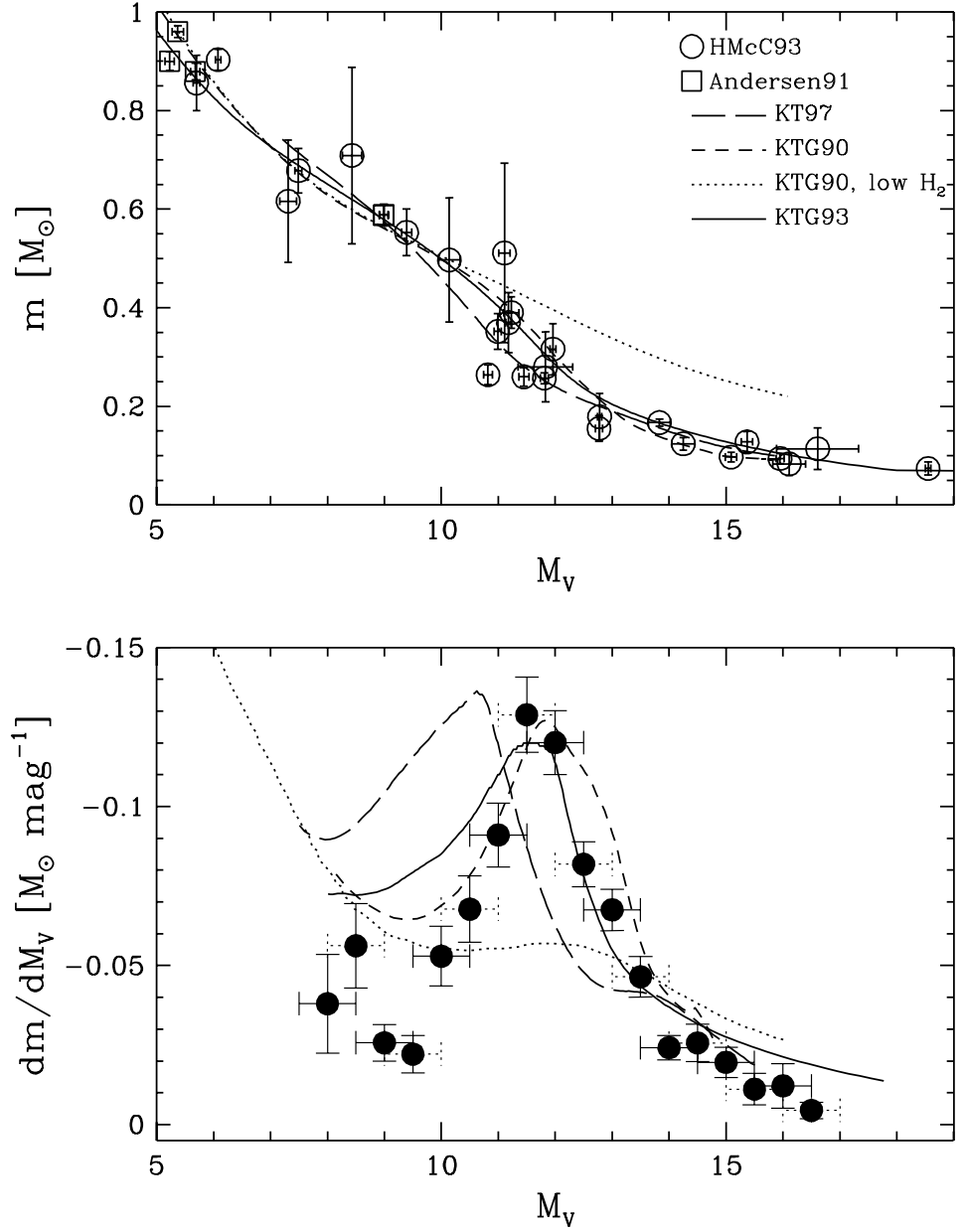


Figure 2. Upper panel: Open circles and squares are observational data as in Fig. 1. The short-dashed and dotted lines are theoretical $m(M_V)$ relations for normal and significantly suppressed H_2 abundance, respectively. More recent models are shown as the long-dashed line. The solid line is the empirical relation. Lower panel: dm/dM_V for the $m(M_V)$ relations shown in the upper panel. The solid dots are $\bar{\psi}_{\text{phot}}$ (Section 6) scaled to fit the figure.

of testing stellar structure theory near the critical $m \approx 0.35 M_{\odot}$ where stars become fully convective. For example, the modern stellar models of KT, that rely on the Eddington approximation for the surface boundary condition, place the minimum in dm/dM_V at too bright an M_V (long-dashed curve in Fig. 2). Treatment of a realistic stellar atmosphere together with the most recent stellar structure physics by Baraffe et al. (1995), leads to improved agreement of the extremum in dm/dM_V with $\bar{\psi}_{\text{phot}}$ (KT). Agreement, however, does not necessarily imply correct physics, as the out-dated models of KTG90 (short-dashed curve in Fig. 2) demonstrates. Theoreticians must, in addition, seek agreement with luminosity–(effective-temperature), colour–magnitude and mass–(absolute-magnitude) relations (KT).

5. Binary Stars

Duquennoy & Mayor (1991, hereinafter DM91) constrain the period distribution and the binary proportion for G-type field stars. The former can be approximated by a Gaussian distribution in $\log_{10}a$ with mean near 34 AU, where a is the semi-major axis. The proportion of binary systems among G-dwarfs is $f_G \approx 0.5 \pm 0.1$. Virtually the same conclusions hold true for K- (Mayor et al. 1992) and M-dwarfs (Fischer & Marcy 1992) (see also Halbwachs, these proceedings, and the summary in Kroupa 1995c). Fisher & Marcy find that about 7 per cent of all M-dwarfs are triple systems, and that about 1 per cent are quadruple systems. The proportions are likely to be higher because the sample of M-dwarf systems within 20 pc is far from complete. The companion star fraction for M-dwarfs is thus $f_{\text{comp,M}} \approx 0.51$ (compare with $f_M = 0.42 \pm 0.09$). Similarly, $f_{\text{comp,G}}$ and $f_{\text{comp,K}}$ is higher than f_G and f_K , respectively. The mass-ratio distribution for G-dwarf binary systems is biased towards low-mass companions (Fig. 10 in DM91). The data are still rather poor for lower-mass primaries but exclude a preponderance of companions with nearly equal mass (Mayor et al. 1992, Fischer & Marcy 1992). How mass-ratio distributions can be miss-interpreted if unknown selection effects operate is shown by Tout (1991).

That deep star-count data are affected significantly if companion stars are not counted has been stressed by Buser & Kaeser (1985), who construct the system LF from the nearby LF (their Fig. 2) and apply it to Galactic structure studies. Piskunov & Malkov (1991) compute the single-star LF given an observed system LF and assumed different mass-ratio distributions, as well as a power-law $m(l)$ relation. In their Fig. 1, they show how the system LF significantly underestimates the stellar number densities. However, the above studies do not include Malmquist bias nor the method of photometric distance estimation.

In deep surveys the typical resolution is 2 arc sec (RG), which implies that multiple stellar systems with dimensions less than 200 AU will not be resolved at a distance of 100 pc. Furthermore, most faint companions will not be seen even if the system is formally resolved because the photometric distance limit decreases with decreasing brightness of the star, and because glare around a bright star can hide faint companions. The great majority of faint companion stars will be missed.

Counting a multiple star system as a single star has the following effects: If the companion(s) are bright enough to affect the system luminosity noticeably,

then the estimated photometric distance will be too small; the remaining companions are lost from the star-count analysis. The former effect enhances the apparent stellar number density at brighter magnitudes. This is countered by the larger effective photometric distance limit together with the approximately exponential stellar density fall-off perpendicular to the Galactic plane. The second effect reduces the star-counts at faint magnitudes leading to a significant bias, because a G-, K- and bright M-dwarf has, on average, a faint M-dwarf companion.

6. Constraining the MF

Before proceeding to infer the MF from the LF, we must understand which information is contained in each of the LFs discussed in Section 2. Clearly, ψ_{near} is the most direct measurement of the MF, given dm/dM_P . But ψ_{near} is poorly constrained for $M_V > 12$ by the small number of stars per magnitude bin, amounting in total to about 20 stars. The constraints available so far suggest that ψ_{near} is approximately flat for $M_V > 12$. The deep surveys show that ψ_{phot} does not vary with direction, so that they can be combined to improve the constraints on ψ_{phot} . However, not all estimates of ψ_{phot} have been treated correctly for Malmquist bias, which depends on the colour–magnitude relation used. To avoid this problem, Kroupa (1995a) combined four photometric LFs that base photometric distance estimation on the $M_V(V - I)$ relation, but are not corrected for Malmquist bias, and obtained $\overline{\psi}_{\text{phot}}^*$. Application of Malmquist corrections then gives an estimate of the distribution of stars with luminosity in the deep surveys, $\overline{\psi}_{\text{phot}}$. This LF implies that 5 stars should have been found in the sampling volume in which ψ_{near} is defined. Given that the one-dimensional velocity dispersion of the stars defining ψ_{near} is about 30 km/sec (KTG93; Reid, Hawley & Gizis 1995), it follows immediately that the chance of observing a local overdensity by a factor of 4 is negligibly small. It is therefore concluded with high confidence that $\overline{\psi}_{\text{phot}}$ and ψ_{near} do not measure the same physical quantity. The same mixing argument explains why ψ_{phot} is independent of direction.

It comes to mind (DLH) that unresolved binary systems are the most likely cause of the significant underdensity of faint stars in $\overline{\psi}_{\text{phot}}$. This has been verified by KTG91. Subsequently, Reid (1991) claimed that binary systems cannot resolve the discrepancy. This, however, is a conclusion drawn upon the basis of assumptions that define models outside solution space (Kroupa 1995b).

In order to clarify some of the questions posed by KTG91 and Reid (1991), KTG93 developed a detailed model of star-count data in which they took into account consistently all the effects discussed above that influence ψ_{phot} . One possible solution is shown in Fig. 3. The upper panel shows the linear $M_V(V - I)$ relation from SIP (solid line), which is taken to be a model for single stars with the same solar-neighbourhood metallicity and age. A realistic distribution of metallicity, age and binarity then leads to a sample of stars that spread around the underlying relation. The systematic colour-dependent off set from the underlying relation is evident. This necessitates a consistent correction of the $M_V(V - I)$ relation fitted to the data. A complex multi-dimensional Monte-Carlo analysis shows that the SIP star count data towards the North Galactic Pole can be fitted with the same MF that also fits ψ_{near} . An exponential Galactic

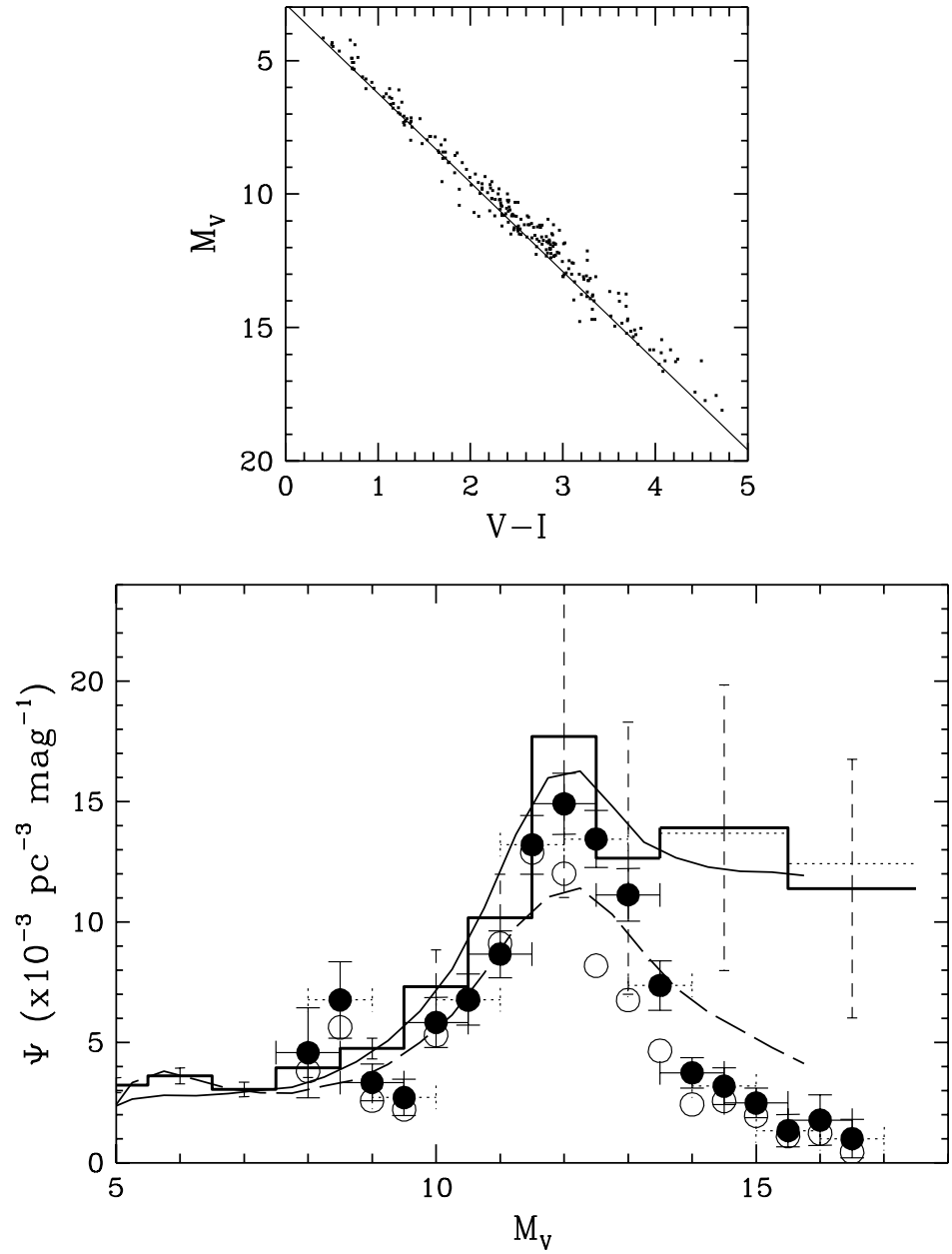


Figure 3. Realistic star-count model. See text for details.

disc, with h a free parameter, is included explicitly, because unresolved metal-rich binary systems with nearly equal component masses at a true distance of 300–400 pc, can enter a photometric distance limit of about 100 pc (Kroupa 1995b).

The resulting MF is approximated by a two-part power-law below $1 M_\odot$. The IMF for all stellar masses is obtained by extension with a third power-law segment for more massive stars from the analysis of Sc:

$$\xi_{\text{KTG}} \propto m^{-\alpha_i},$$

where $0.70 < \alpha_1 < 1.85$ for $0.08 < m/M_\odot \leq 0.5$, $\alpha_2 = 2.2$ for $0.5 < m/M_\odot \leq 1$, and $\alpha_3 \approx 2.7$ for $1 < m/M_\odot$ (Fig. 22 and Eqn. 13 in KTG93). In this notation Salpeter’s power-law index is $\alpha = 2.35$. There is some evidence that $\alpha_3 < 2.7$ for the IMF (Tsujiimoto et al. 1997 and references therein), and for main-sequence stars in the Galactic field $\alpha_3 \approx 4.5$.

The model *observed* single-star LF becomes the solid curve in the lower panel of Fig. 3. It is affected significantly by the spread of metallicities and trigonometric distance uncertainties, and compares very well with the real ψ_{near} shown as the solid histogram (from Kroupa 1995a). The thin dotted histogram shows the effect of counting Gl 866C and shifting the sampling distance from 5.2 pc to 5.23 pc. The dashed curve is the model photometric LF with Malmquist bias not removed, assuming a companion star fraction $f = 0.7$ and $h = 270$ pc. The solid dots show $\bar{\psi}_{\text{phot}}^*$ (binned into one-magnitude wide bins offset by half a magnitude), which is the relevant observational constraint, and the open circles are $\bar{\psi}_{\text{phot}}$.

In the above model, stars are combined randomly from the IMF to make the uncorrelated mass ratio distribution, f_q , for binary systems. This procedure does not give an f_q that is consistent with the observational constraints (Section 5) because too many low-mass companions are produced. That the MF derived with the above analysis remains a good solution if f_q consistent with the observational constraints is used, is shown in Fig. 4. In the upper left panel (m_S and m_P are the mass of the secondary and primary, respectively) the model f_q for G-dwarf primaries is the solid histogram, which can result from the initial uncorrelated distribution (dot-dashed histogram) if stars form in embedded clusters (Kroupa 1995d). The observed data (DM91) are the solid dots. The overall binary proportion is $f = 0.48$. Of these about 9 per cent have periods shorter than 10^3 d, with f_q given by the solid histogram in the upper right panel of Fig. 4. The observed data (Mazeh et al. 1992) are the solid dots. The model f_q for all primaries less massive than $1.1 M_\odot$ and all periods is shown in Fig. 12 in Kroupa (1995d). The single star LF for a population with equal metal abundance, age and no distance errors is the solid curve in the lower panel of Fig. 4 (compare to Fig. 3). The corresponding system LF is the dashed curve, and the relevant observational data are the solid dots ($\bar{\psi}_{\text{phot}}$).

Comparison of Figs. 3 and 4 shows that the model photometric LFs contain too many systems for $M_V > 14$. As discussed in Kroupa (1995b), this is not to be taken too seriously because, among other effects, photometric calibration may be uncertain for the faint red dwarfs. J. Gizis (private communication) points out that the hitherto neglected non-linearity of the $M_V(V - I)$ relation (Section 4 in Leggett, Harris & Dahn 1994; Fig. 1 in Baraffe et al. 1995) increases

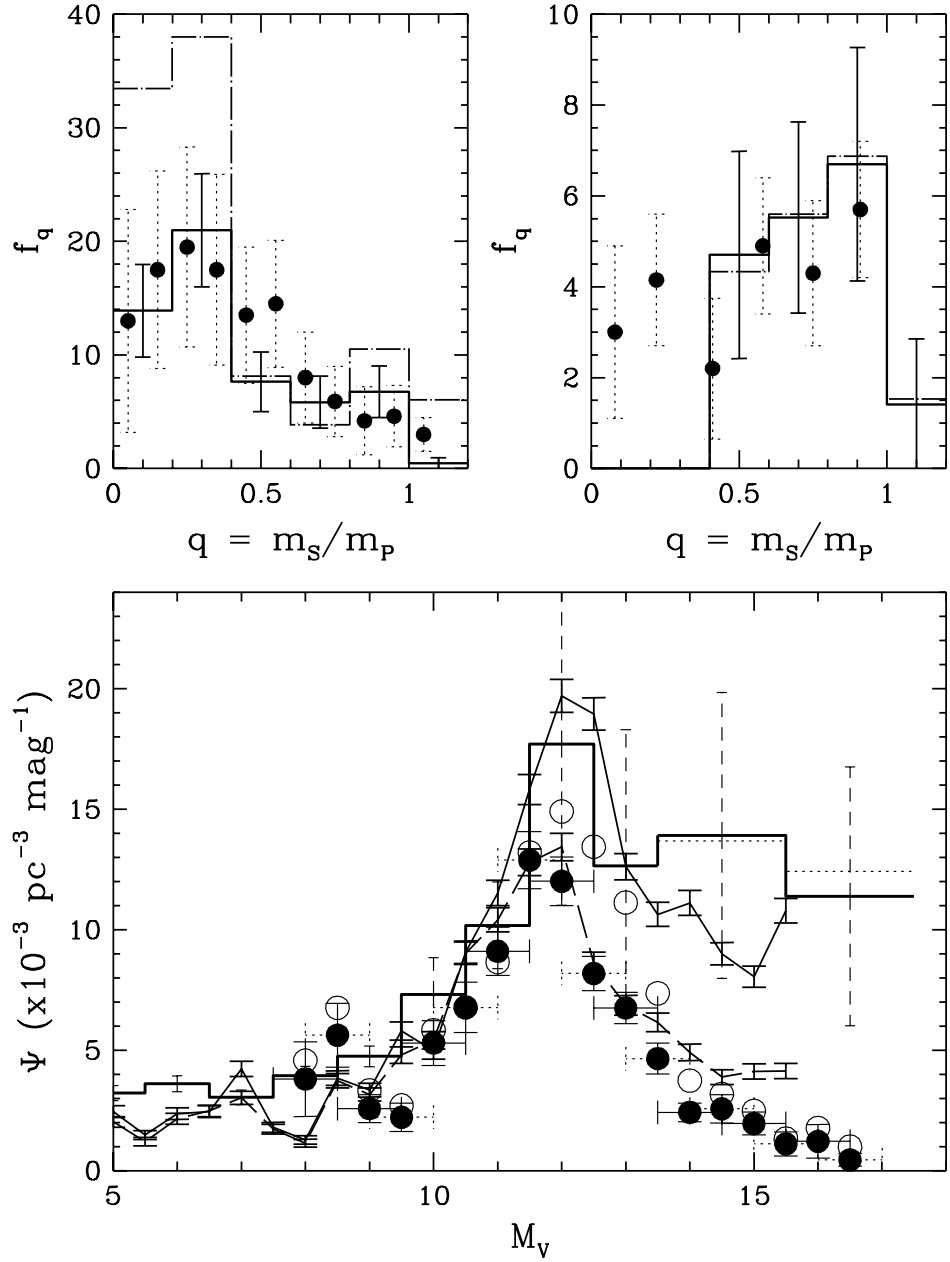


Figure 4. Realistic binary star model. See text for details.

ψ_{phot} at the faint magnitudes, which improves agreement with the models. The model shown in Fig. 4 does not rely on adoption of a colour-magnitude relation.

It is thus possible to unify ψ_{near} and ψ_{phot} . The above analysis leads to the most stringent constraints on the MF available because both the single-star (i.e. ψ_{near}) and the much better constrained system LF (i.e. ψ_{phot}) are used simultaneously. Nevertheless, the most direct path to the MF is via the single-star LF. Only a major, careful and time-consuming observational effort (e.g. Henry et al. 1997) will improve the poorly constrained ψ_{near} , but it is instructive to consider the MF that results from the direct conversion (see Section 1) of the presently available ψ_{near} using different $m(M_P)$ relations: D’AM86 find $1.64 < \alpha < 2.44$ for $0.1 < m/M_\odot < 0.3$ using the Wielen et al. (1983) LF and their theoretical mass–luminosity relation; HM90 find $\alpha \approx 0.8$ for $0.08 < m/M_\odot < 0.5$ using the nearby LF they estimate in the K-band and their empirical $m(M_K)$ relation; Laughlin & Bodenheimer (1993) find $\alpha \approx 2.35$ for $0.1 < m/M_\odot < 0.5$ using $\psi_{\text{near}}(M_K)$ from HM90 and their own mass–luminosity relation; Haywood (1994) finds $1.3 < \alpha < 2.3$ for $0.12 < m/M_\odot < 0.35$ using $\psi_{\text{near}}(M_V)$ from DLH and stellar models from VandenBerg; Kroupa (1995b) finds $0.66 < \alpha_1 < 1.44$ for $\psi_{\text{near}}(M_V)$ and $m(M_V)$ from KTG93; and Mera et al. (1996) find $\alpha \approx 2 \pm 0.5$ for $m < 0.6 M_\odot$ using ψ_{near} from KTG93 and their own $m(M_V)$ relation. Clearly, more or less the same estimate for the single-star LF, ψ_{near} , yields quite different results depending on which mass–luminosity relation is used. Another major source of bias in all these estimates of the MF is the neglect of the metallicity spread and parallax errors. This is demonstrated by comparing $0.66 < \alpha_1 < 1.44$ (Fig. 3 in Kroupa 1995b) with the model that does include these effects: $0.6 < \alpha_1 < 2.3$ (Fig. 16 in KTG93).

An entirely independent estimate of the MF is provided by Tsujimoto et al. (1997), who find $\alpha > 1.8$ down to below the hydrogen burning mass limit using a model for the chemical enrichment history of the Galaxy, and the additional constraint given by the mass-to-light ratio of stars in the solar neighbourhood. Finally, it is interesting to note that Zhao, Rich & Spergel (1996) construct a consistent model of the Galactic bar, and compare the distribution of microlensing time-scales with predictions assuming different stellar MFs. Their Fig. 3 shows that it is possible to obtain reasonable agreement with the distribution of time-scales if the MF is flat below $0.5 M_\odot$ ($\alpha = 0$; but see Chabrier, these proceedings), and also if it continues as a Salpeter ($\alpha = 2.35$) power-law to lower masses, as long as there is no significant population of brown dwarfs.

7. Discussion and Conclusions

Below approximately $0.5 M_\odot$ the IMF may be conveniently approximated by a power law with $\alpha \approx 1.5$ down to the hydrogen burning mass limit (see also Larson 1992). Whether the MF continues as some log-normal function to smaller masses (e.g. Zinnecker 1984; Adams, these proceedings) cannot yet be decided upon (see also Malkov, Piskunov & Shpil’kina 1997).

Main-sequence stars ($\alpha_3 = 4.5$) contribute $\Sigma_* = 30 \pm 8 M_\odot \text{ pc}^{-2}$ to the Oort limit for the three-part power-law MF with $0.7 < \alpha_1 < 1.85$ and $h \approx 300 \text{ pc}$. The inter-stellar medium contributes $\Sigma_{\text{ISM}} = 13 \pm 3 M_\odot \text{ pc}^{-2}$ (Kuijken & Gilmore 1989) and stellar remnants contribute $\Sigma_{\text{rem}} = 4.5 \pm 1.5 M_\odot \text{ pc}^{-2}$ (Weidemann

1990). It follows that the dynamically inferred mass-density in the Galactic disc ($\Sigma_* = 48 \pm 9 M_\odot \text{ pc}^{-2}$, Kuijken & Gilmore 1991) can be accounted for. It also follows that dark matter, e.g. in the form of brown dwarfs, cannot be a significant mass-component. The steeper MFs discussed in Section 3 imply essentially the same Σ_* (Mera et al. 1996), but it remains to be seen if such MFs can also fit $\bar{\psi}_{\text{phot}}$. For this, detailed modelling (Section 6) is required. Care must be taken to ensure that a $m(M_P)$ relation is used that fits the observational constraints (Fig. 2), that its first derivative is continuous, and that it is defined on an adequately fine stellar-mass grid (KT).

LFs extending down to approximately the hydrogen burning mass limit have been observed for the young Pleiades (Hambly, Hawkins & Jameson 1991) and the dynamically evolved Hyades (Reid 1993) clusters. The power-law MF for Galactic field stars with $\alpha_1 = 1.3$ fits both LFs (Kroupa 1995e). Observed LFs must be corrected consistently for unresolved binary stars, but care must be taken not to assume the same binary-star orbital characteristics in open clusters as in the Galactic field. The Pleiades and Hyades clusters are not typical reservoirs of Galactic field stars, so there does not appear to be much evidence for an environmentally dependent IMF for low-mass stars.

Acknowledgments. I am grateful to Michael Hawkins for a very memorable evening ten years ago at the Siding Spring Observatory, where he gave me my first introduction to this subject. I thank C. A. Tout for proof-reading the manuscript.

References

- Andersen, J., 1991, A&AR, 3, 91
 Baraffe, I., Chabrier, G., Allard, F., & Hauschildt, P. H., 1995, ApJ, 446, L35
 Basri, G. & Marcy, G. W., 1997, in Star Formation: Near and Far, Holt, S., Maryland
 Bessell, M. S. & Stringfellow, G. S., 1993, ARA&A, 31, 433
 Buser, R. & Kaeser, U., 1985, A&A, 145, 1
 Chabrier, G. & Baraffe, I., 1997, A&A, in press
 Dahn C. C., Liebert, J., Harrington R. S., 1986, AJ, 91, 621 (DLH)
 D'Antona, F. & Mazzitelli, I., 1983, A&A, 127, 149 (D'AM83)
 D'Antona, F. & Mazzitelli, I., 1986, A&A, 162, 80 (D'AM86)
 Duquennoy, A. & Mayor, M., 1991, A&A, 248, 485 (DM91)
 Fischer, D. A. & Marcy, G. W., 1992, ApJ, 396, 178
 Gilmore, G., Reid, N., & Hewett, P., 1985, MNRAS, 213, 257
 Hambly, N. C., Hawkins, M. R. S., & Jameson, R. F., 1991, MNRAS, 253, 1
 Hawkins, M. R. S. & Bessell, M. S., 1988, MNRAS, 234, 177
 Haywood, M., 1994, A&A, 282, 444
 Haywood, M., Robin, A. C., & Cr ez e, M., 1997, A&A, 320, 428
 Henry, T. J. & McCarthy, D. W., 1990, ApJ, 350, 334 (HM90)
 Henry, T. J. & McCarthy, D. W., 1993, AJ, 106, 773 (HM93)

Henry, T. J., Ianna, P. A., Kirkpatrick, J. D., & Jahreiss, H., 1997, *AJ*, in press

Jahreiss, H., 1994, in *Science with Astronomical Near-Infrared Sky Surveys*,
 Epchtein, N., Omont, A., Burton, B., & Persi, P., Kluwer: Dordrecht, 63

Jarrett, T. H., Dickman, R. L., & Herbst, W., 1994, *ApJ*, 424, 852

Kirkpatrick, J. D., McGraw, J. T., Hess, T. R., Liebert, J., & McCarthy, D. W.,
 1994, *ApJS*, 94, 749

Kirkpatrick, J. D., Henry, T. J., & Irwin, M. J., 1997, *AJ*, 113, 1421

Kroupa, P., 1995a, *ApJ*, 453, 350

Kroupa, P., 1995b, *ApJ*, 453, 358

Kroupa, P., 1995c, *MNRAS*, 277, 1491

Kroupa, P., 1995d, *MNRAS*, 277, 1507

Kroupa, P., 1995e, *MNRAS*, 277, 1522

Kroupa, P. & Tout, C. A., 1997, *MNRAS*, 287, 402 (KT)

Kroupa, P., Tout, C. A. & Gilmore, G., 1990, *MNRAS*, 244, 76 (KTG90)

Kroupa, P., Tout, C. A. & Gilmore, G., 1991, *MNRAS*, 251, 293 (KTG91)

Kroupa, P., Tout, C. A. & Gilmore, G., 1993, *MNRAS*, 262, 545 (KTG93)

Kuijken, K. & Gilmore, G., 1989, *MNRAS*, 239, 605

Kuijken, K. & Gilmore, G., 1991, *ApJ*, 367, L9

Larson, R. B., 1992, *MNRAS*, 256, 641

Laughlin, G. & Bodenheimer, P., 1993, *ApJ*, 403, 303

Leggett, S. K. & Hawkins, M. R. S., 1988, *MNRAS*, 234, 1065

Leggett, S. K., Harris, H. C., & Dahn, C. C., 1994, *AJ*, 108, 944

Malkov, O. Yu., Piskunov, A. E., & Shpil’kina, D. A., 1997, *A&A*, 320, 79

Mayor, M., Duquennoy, A., Halbwachs, J.-L., & Mermilliod, J.-C., 1992, in
Complementary Approaches to Double and Multiple Star Research, IAU
 Colloqu. 135, McAlister, H. A. & Hartkopf, I., San Francisco: ASP, Vol.
 32, 73

Mazeh, T., Goldberg, D., Duquennoy, A., & Mayor, M., 1992, *ApJ*, 401, 265

Méra, D., Chabrier, G., & Baraffe, I., 1996, *ApJ*, 459, L87

Miller, G. E. & Scalo, J. M., 1979, *ApJS*, 41, 513 (MS)

Piskunov, A. E. & Malkov, O. Yu., 1991, *A&A*, 247, 87

Reid, N., 1991, *AJ*, 102, 1428

Reid, N., 1993, *MNRAS*, 265, 785

Reid, N. & Gilmore, G., 1982, *MNRAS*, 201, 73 (RG)

Reid, N., Hawley, S. L., & Gizis, J. E., 1995, *AJ*, 110, 1838

Santiago, B. X., Gilmore G., Elson, R. A. W., 1996, *MNRAS*, 281, 871

Scalo, J. M., 1986, *Fundam. Cosmic Phys.*, 11, 1 (Sc)

Simons, D. A., Henry, T. J., & Kirkpatrick, J. D., 1996, *AJ*, 112, 2238

Stobie, R. S., Ishida, K., & Peacock, J. A., 1989, *MNRAS*, 238, 709 (SIP)

Tinney, C. G., Reid, I. N., Mould, J. R., 1993, *ApJ*, 414, 254

Tout, C. A., 1991, *MNRAS*, 250, 701

- Tsujimoto, T., Yoshii, Y., Nomoto, K., Matteucci, F., Thielemann, F.-K., & Hashimoto, M., 1997, *ApJ*, in press
- Ugoren, A. R. & Armandroff, T. E., 1981, *AJ*, 86, 1898
- Weidemann, V., 1990, in *Baryonic Dark Matter*, Lynden-Bell, D., & Gilmore, G., Dordrecht: Kluwer, 87
- Wielen, R., Jahreiss, H., & Krüger, R., 1983, in *The Nearby Stars and The Stellar Luminosity Function*, Davis Philip, A. G., Ugoren, A. R., IAU Colloq. No. 76, New York: Davis Press, 163
- Zhao, H. S., Rich, R. M., & Spergel, D. N., 1996, *MNRAS*, 282, 175
- Zinnecker, H., 1984, *MNRAS*, 210, 43